DOI: 10.1002/anie.201404483

Nanopatterns

Controlling the Orientation of Nanowrinkles and Nanofolds by Patterning Strain in a Thin Skin Layer on a Polymer Substrate**

*Mark D. Huntington, Clifford J. Engel, and Teri W. Odom**

Dedicated to Professor George M. Whitesides on the occasion of his 75th birthday

Abstract: *We describe herein how to control the orientation of polymer nanowrinkles and nanofolds with large amplitudes. Nanowrinkles were created by chemically treating thermoplastic polystyrene sheets to form a thin skin layer and then heating the substrate to relieve strain. By manipulating the strain globally and locally in the skin layer, we could tune whether wrinkles or folds formed, as well as the distances over which these structures could be produced. This unique materials system provided access to high strain regimes, which enabled mechanisms behind the spontaneous formation of complex structures to be explored.*

Over every length scale, wrinkles form when a compressive strain is applied to a stiff skin on a soft substrate.[1] The average wrinkle periodicity (λ) can be predicted from the skin thickness (h) and the ratio of the Young modulus of the skin (E_S) and substrate (E_B).[1–3] For microscale and nanoscale wrinkles, the skin layer is typically a stiffened polymer or deposited metal film, whereas substrate examples include compressible polymers or fluids.[2,4–7] Wrinkling has emerged as a way to control the mechanical, electrical, and optical properties of a substrate without changing the bulk properties of the material.[3,4] For example, polymer microwrinkles can increase hydrophobicity while maintaining mechanical flexibility.[8] We previously reported how the wavelengths of nanowrinkles ($\lambda < 500$ nm) could be tuned down to 30 nm by creating a skin layer on thermoplastic polystyrene (PS) sheets through plasma treatment with fluorinated gases.[9] This chemical patterning method enabled access to wrinkle wavelengths much smaller than those accessible with other systems[1,9] because of the low Young's modulus ratio ($E_S/E_B < 10$) and thin skin layers ($h < 20$ nm).

Besides λ, wrinkle amplitude (A) is another important parameter that defines the properties of a substrate. Uniformly distributed 2D strain results in randomly oriented nanowrinkles with a value A that depends on the amount of applied strain (ε) until a critical threshold is reached. In this strain regime, A has been limited to less than 10 nm for nanowrinkles.[1,4] Above this threshold, strain is relieved by the formation of a second generation of wrinkles with a larger periodicity[4] or by a wrinkle-to-fold transition,[5,10] whereby strain is concentrated into periodic folds.[7,11] Such structures that form under high strain may enable additional tuning of surface properties; however, the materials characteristics that lead to these structures are not well understood.[3] Patterning of the local strain distribution in the skin layer at the microscale is another strategy to create ordered structures from inherently disordered patterns.[2,12–16] For example, etched features in a gold skin layer on a poly(dimethylsiloxane) substrate have been used to orient microwrinkles over distances up to 17 times the wrinkle wavelength.[2,12] Although micro- and nanoscale patterns[17] have been used to control the amplitude and wavelength of microscale wrinkles, macroscale control over the local orientation of nanowrinkles has not been reported. The two major barriers to the creation of ordered nanowrinkles are 1) the limited skin/substrate materials systems that can generate wrinkles at sub-100 nm length scales; and 2) challenges in fabricating large ($> \text{cm}^2$) areas of nanopatterns on elastomeric substrates.

Herein we show that the amplitude and orientation of nanowrinkles can be tuned by patterning strain in the stiff skin layer of thermoplastics. First, we produced one-dimensional (1D) and two-dimensional (2D) nanowrinkles in PS sheets with aspect ratios of approximately 1. Such a high λ/A ratio was possible because we could mitigate the effects of nonlinear strain between the skin and substrate by forming wrinkles at high temperatures (above the glass-transition temperature, T_g). Second, we characterized changes in wrinkle wavelength and amplitude with increased strain and found that both linear and nonlinear effects were present. At high strain ($\varepsilon > 0.6$), we observed the formation of nanofolds and hierarchical wrinkle structures, which indicated that strain in the skin layer dictated the types of secondary structures that could form. Finally, we found that we could control the orientation of nanowrinkles by manipulating both local and global strain distributions in the skin layer. To

[*] M. D. Huntington, Prof. T. W. Odom
Department of Materials Science and Engineering
Northwestern University
2145 Sheridan Road, Evanston, IL 60208 (USA)
C. J. Engel, Prof. T. W. Odom
Department of Chemistry, Northwestern University
E-mail: todom@northwestern.edu
Homepage: http://chemgroups.northwestern.edu/odom

[**] This research was supported by the National Science Foundation (CMMI-1069180, patterning holes), the Office of Naval Research (N00014-13-1-0172, nanowrinkle process), and the Argonne-Northwestern Solar Energy Research (ANSER) Center (DE-SC0001059, wavelength studies). It was conducted with Government support under Grant FA9550-05-C-0059 (M.D.H., 32 CFR 168a). M.D.H. and C.J.E. acknowledge support from a Ryan Fellowship. For these studies, we made use of the NUANCE Center facilities, which are supported by NSF-MRSEC, NSF-NSC, and the MRSEC (Grant DMR-1121262).

Supporting information for this article is available on the WWW under http://dx.doi.org/10.1002/anie.201404483.

quantify the ordering, we developed two different methods to characterize the average orientation. Physical patterning of the skin layer prior to nanowrinkle formation enabled the creation of wrinkle patterns that were 1000 times smaller than any previously reported.

Figure 1 shows how wrinkle amplitude changed with applied strain for PS nanowrinkles. In brief, nanowrinkles were formed by treating a PS sheet with reactive ion etching (RIE) plasmas followed by heating to apply strain and shrink

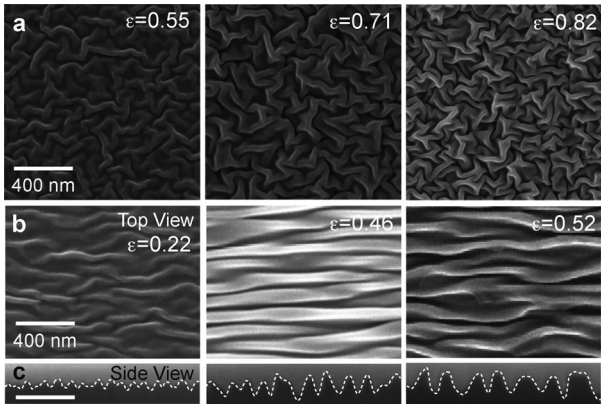

Figure 1. Application of strain to control the amplitude of 1D and 2D nanowrinkles. a,b) SEM images of 2D (a) and 1D nanowrinkles (b) under three different strains (ε). c) Cross-sections of 1D nanowrinkles cut by focused ion beam (FIB) milling (scale bar: 400 nm).

the substrate.[9] By this method, the wrinkle wavelength could be continuously varied from $\lambda = 30$ to 500 nm by changing the plasma gas or RIE exposure time.[9] In this study, we focused on a specific set of conditions (exposure time: $t = 30$ s; gas: CHF_3) that resulted in nanowrinkles with $\lambda \approx 150$ nm. We controlled the amount of strain applied to the system by varying the amount of time that the PS films were heated above T_g (see the Experimental Section). For 2D nanowrinkles, the strain could be varied continuously from $\varepsilon = 0$ to 0.82 without the formation of self-similar wrinkles or folds (Figure 1a). We obtained 1D nanowrinkles by allowing the sample to shrink in only one direction (Figure 1b; see also Figure S1 in the Supporting Information). Thus, we could tune the average orientation of wrinkles by manipulating the applied strain distribution.

An isotropic 2D compressive strain ($\varepsilon_x = \varepsilon_y$) produces random wrinkle orientations;[14] however, if strain anisotropy is introduced, the distribution of wrinkle order changes. Within the limit of 1D strain, all wrinkles align perpendicular to the applied strain.[14] The order parameter (S), which varies from 0 (completely random) to 1 (perfectly ordered), is typically used to quantify the orientational order of wrinkles.[18] The parameter S varies with different anisotropic strains from approximately 0.4 for 2D isotropic strain to approximately 0.98 for 1D strain (see Figure S2). The S value was determined by processing the SEM image (see Figure S2a) by using MATLAB functions to determine the orientation of wrinkle peaks. This method is subject to image-processing errors because the orientation depends on the black-and-white-conversion threshold (see Figure S2b). Hence, we developed a new order parameter (S_{FFT}) based on the angular spread of the fast Fourier transform (FFT) of the SEM image (see the Supporting Information). The parameter S_{FFT} follows a trend similar to that of S for different anisotropic strains with ranges from approximately 0.04 for 2D isotropic strain to approximately 0.77 for 1D strain (see Figure S2c). The S_{FFT} values were slightly lower than those for S, thus indicating that S_{FFT} could detect smaller variations in highly ordered structures. This sensitivity makes the S_{FFT} parameter a better metric for the study of small changes in systems that can generate highly ordered features, such as 1D nanowrinkles. We found that neither S nor S_{FFT} varied significantly with absolute applied strain (see Figure S3).

We measured the amplitude of 1D nanowrinkles by evaluating focused ion beam (FIB) milled cross-sections over a range of strain ($\varepsilon = 0$–0.52) similar to that used for 2D nanowrinkles (Figure 1c). Since 1D nanowrinkles have S and S_{FFT} values that approach 1, a cross-section along the strain direction can provide an accurate representation of wrinkle wavelength, amplitude, and curvature. For the sample with the largest strain ($\varepsilon = 0.52$; Figure 1b), we measured an amplitude $A = 141$ nm (Table 1), which is 3–10 times greater than any amplitude reported for 1D or 2D nanowrinkles.[1,5] Wrinkle curvature was determined by taking the second derivative of the wrinkle trace (Figure 1c) and was found to increase with strain.

Table 1: Amplitude and aspect ratio of 1D wrinkles with different amounts of strain.

ε	A [nm]	λ [nm]	Aspect ratio	Curvature [nm^{-1}]
0.22 ± 0.005	28 ± 1	189 ± 5	0.15 ± 0.02	0.016 ± 0.005
0.46 ± 0.009	93 ± 1	158 ± 5	0.59 ± 0.04	0.029 ± 0.008
0.52 ± 0.005	141 ± 1	151 ± 5	0.94 ± 0.10	0.039 ± 0.015

As strain grows beyond a threshold, there are two mechanisms to describe how the system responds.[1,2,19,20] In the linear model,[11] the additional strain is absorbed by increasing A while keeping λ constant (Figure 2a). This model best describes characteristics of wrinkles at relatively low strain ($\varepsilon < 0.1$). In the nonlinear model,[11] strain can be absorbed by decreasing λ while keeping A constant (Figure 2b). At high strain, A is a more complicated function of strain and has been described by a polynomial expansion (see Figure S4). Since high strain ($\varepsilon \leq 0.6$, for 1D) is possible in our PS system without the formation of secondary structures, we expected that nonlinear effects would be important for understanding changes in λ and A. The wavelength of 1D nanowrinkles in Figure 1 decreased with increasing strain (Figure 2c). The relationship between λ and A—whereby A increased while λ decreased—fell in between the corresponding relationships for the linear and nonlinear models. For comparison, we calculated the change in curvature for both linear and nonlinear models (see Figure S5). For 2D nanowrinkles, we also found that the wrinkle wavelength decreased linearly with applied strain (see Figure S6); however, 2D wrinkles cannot be directly compared to these

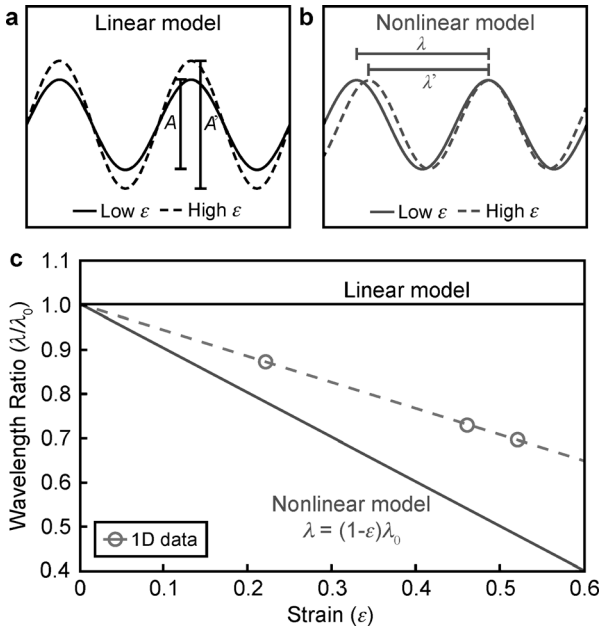

Figure 2. Linear and nonlinear characteristics of PS nanowrinkles. a,b) Schematic representation of how strain is absorbed by the stiff skin in the linear (a) and nonlinear model (b). c) The change in wavelength as a function of strain fell between the corresponding functions for the linear and nonlinear models. The slope was fit to $\lambda = (1-\alpha\varepsilon)\lambda_0$, in which $\alpha = 0.59$.

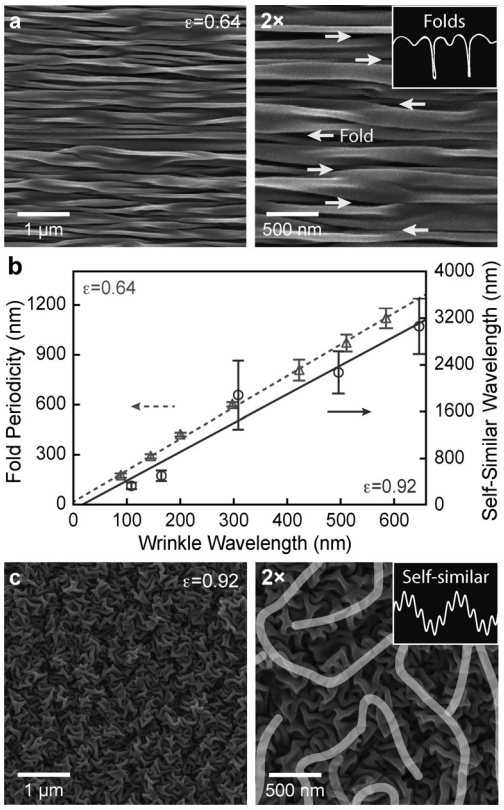

Figure 3. Formation of nanofolds and self-similar wrinkles from PS nanowrinkles under high strain. a) Formation of nanofolds by 1D nanowrinkles at high strain. Inset: Cross-section of nanofolds. b) Plot of fold and self-similar-wrinkle periodicity as a function of wrinkle wavelength. Error bars represent one standard deviation from approximately 250 measurements. c) Formation of self-similar wrinkles by 2D nanowrinkles at high strain. Inset: Cross-section of self-similar wrinkles.

models because the strain in two dimensions is defined differently from that in one dimension.

For 1D wrinkles at high strain ($\varepsilon > 0.6$), folds started to form across the surface (Figure 3a); the strain was concentrated into a single fold, and the surrounding wrinkles decreased in amplitude. On the basis of previous studies, it was proposed that either large Young moduli or a small bending stiffness ($B = h^3 E_S$) might cause the formation of folds instead of self-similar winkles.[5,7,11] The elastic properties of the substrate could also play a role in the topography of the secondary structures.[21] For example, viscous substrates (e.g. water or uncured polymers) can produce deeper folds at periodicities much larger than those observed for elastic substrates.[21] To evaluate substrate effects, we measured the Young modulus, E_{PS}, as a function of temperature by using a triboindenter. The E_{PS} value drastically decreased at $T > T_g$ (see Figure S7). This reduction in stiffness was expected, since at these temperatures, PS should become viscoelastic.[22]

Neither the skin nor the substrate properties could be independently measured above T_g. In a previous study, however, we extracted the ratio E_S/E_B by measuring the change in wrinkle wavelength (λ) as a function of skin thickness (h). The extracted ratio E_S/E_B for this PS system was < 10,[9] which is much smaller than the proposed thresholds for fold formation ($100 < E_S/E_B < 10^4$).[5] Also, at low E_S/E_B ratios (< 100), wrinkles are predicted to increase in amplitude instead of forming folds.[5] One explanation for this difference in our PS system might be that h (ca. 20 nm), and as a result the small B value, has an influence on fold formation.[11] Therefore, we tested effects of the bending stiffness, B, by measuring fold periodicity for different values of h. Surprisingly, we found that folds occurred even when B was varied by several orders of magnitude. We also found that fold periodicity increased linearly with increasing h at a rate of two times the increase in the nanowrinkle wavelength (Figure 3b), which provides additional evidence that the fold characteristics did not depend on B.

We expected the viscoelastic properties of the substrate, the E_S/E_B ratio, and the B value to be similar for 1D and 2D nanowrinkles; however, for 2D nanowrinkles, when the strain was increased above $\varepsilon = 0.9$, a second generation of wrinkles (self-similar) formed with a periodicity about 5 times the wrinkle wavelength, instead of nanofolds (Figure 3b,c). The mechanical properties of the skin and the substrate cannot fully explain the trends we observed. Instead, the direction (1D or 2D) of strain distribution in the skin seemed to play a dominant role in determining how the secondary strain was relieved. One explanation for the different types of secondary structure produced under 2D strain is that the interweaving of 2D nanowrinkles prevents folds from forming during the wrinkling process.

To examine whether the generation of new nanotextures or the ordering of wrinkles or folds was also possible by locally controlling the strain distribution, we patterned strain-relief features in the skin layer (Figure 4a). Strain-relief

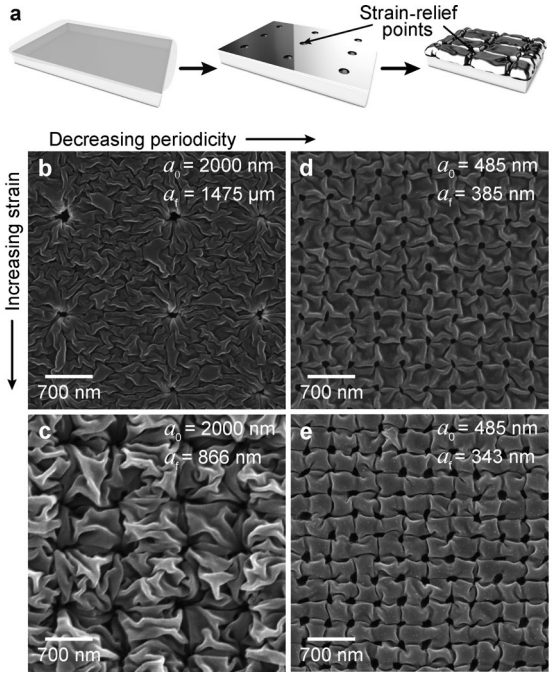

Figure 4. Production of oriented wrinkle patterns by patterning of the strain through the introduction of holes in the skin layer. a) Schematic illustration of the fabrication of strain-relief features. Briefly, PS was treated with a CHF_3 plasma, strain-relief features were then etched into the PS through a Cr hole-array mask in a second RIE step, the Cr mask was removed, and the sample was heated to form wrinkles. b–e) SEM images of nanowrinkle samples with square arrays of strain-relief features with the periodicities indicated. b) $a_0' = 2$ μm, $a_f' = 1475$ nm; c) $a_0' = 2$ μm, $a_f' = 866$ nm; d) $a_0 = 485$ nm, $a_f = 385$ nm; e) $a_0 = 485$ nm, $a_f = 343$ nm.

points were formed by physically etching holes (ca. 100 nm deep) in the PS film through a metal hole-array mask in a second RIE step (see Experimental Section). It has previously been shown that patterning of the local strain distribution in the skin at the microscale can be used to control the orientation of wrinkles at small strains.[2,12,16] By using inverse solvent-assisted nanoscale embossing (inSANE),[23] we generated strain patterns with periodicities that were close to the wrinkle wavelength. We investigated the effects of patterned strain-relief points on wrinkle formation at this length scale by etching square arrays of holes with two periodicities: one close to λ ($a_0 = 4\lambda$), and one much larger than λ ($a_0' = 13\lambda$). The larger spacing was selected to test how isolated holes could direct local wrinkle orientation, and the smaller periodicity was chosen to test how strain distribution changed when the hole periodicity was close to λ. We studied both spacings at low strain ($\varepsilon \approx 0.4$) and high strain ($\varepsilon \approx 0.8$) to examine whether the strain-relief patterns affected the secondary structures. For the larger periodicity (a_0') holes, at $\varepsilon = 0.45$ ($a_0' = 2$ μm; final periodicity, $a_f' = 1.475$ μm), the nanowrinkles were oriented radially around the etched holes (Figure 4b), in a pattern similar to that surrounding a single point (see Figure S8). At higher strain ($\varepsilon = 0.8$), the periodicity of the holes was reduced from $a_0 = 2000$ nm to $a_f = 866$ nm ($a_f \approx 6\lambda$), and a self-similar wrinkle structure was formed (Figure 4c). The self-similar wavelength closely matched the final periodicity of the 2D pattern, and the secondary wrinkles were oriented along the 2D square lattice (see Figure S9).

When the periodicity of the strain-relief points was reduced to $a_0 = 485$ nm and a small strain was applied ($\varepsilon = 0.36$; $a_f = 385$ nm), the wrinkles began to align between the etched holes, and shallow folds began to form (Figure 4d). At a slightly higher strain ($\varepsilon = 0.51$; $a_f = 343$ nm), the wrinkles collapsed into deeper folds along the four sides of the square pattern (Figure 4e). Therefore, we found that the periodicity of the strain-relief patterns must be around 2–3 times the wrinkle wavelength, λ, (after shrinking) for folds to form. To provide additional support for this result, we reduced the λ value from 150 to 70 nm and examined the effects of relief points with three different multiples of λ ($a_0 \approx 17\lambda$, 8λ, and 6λ). For the two larger periodicities ($a_0 = 1200$ and 600 nm), no folds formed (see Figure S10a,b); however, when the strain-relief pattern was reduced to $a_0 = 400$ nm ($a_0 \approx 6\lambda$, but ca. 3λ after shrinking), nanofolds again appeared (see Figure S10c). Hence, by engineering both the strain-relief periodicity and the wrinkle wavelength, we could create oriented folds with tunable orientation, amplitude, and density.

Besides investigating how periodic arrays of holes in the skin layer can create isolated points of strain relief, we also examined the effects of larger perturbations. Etched line patterns with varying widths (w) and periodicities (a_0) were created in the stiffened skin layer by a procedure similar to that for the formation of the holes in Figure 4. Upon shrinking the treated PS substrate in two dimensions, nanowrinkles formed perpendicular to the physically etched lines (Figure 5). Similar to the square array in Figure 4e, when the periodicity of the lines was about 2λ, we observed the formation of folds at high strain ($\varepsilon = 0.52$; Figure 5a). For the larger line periodicities at high strain ($\varepsilon \approx 0.68$), the wrinkle amplitude increased, but no folds were formed (Figure 5b,c).

Lines of strain relief reduced the magnitude of compressive strain experienced by the skin (as compared to that experienced with points of strain relief), which resulted in a corresponding reduction of wrinkle amplitude. This effect was especially apparent at low strain ($\varepsilon = 0.29$) in the smallest-periodicity line patterns (Figure 5d), for which $a_0 = 500$ nm and $w = 250$ nm. When the periodicity of the lines increased ($a_0 = 3$ μm, $w = 1.5$ μm), the amplitude of the nanowrinkles also increased at the same strain ($\varepsilon = 0.31$) because there were fewer etched lines, and therefore there was less strain relief per area (Figure 5e). At a larger width w (2.5 μm; Figure 5f), nanowrinkles were not all oriented perpendicular to the patterned lines, especially in the center. Notably, strain-relief features can influence wrinkle orientation over distances greater than 30 times the wrinkle wavelength (Figure 5c–f). To determine the upper limit over which nanowrinkles could be aligned, we patterned 25 μm lines spaced by 50 μm (see Figure S11). We found that wrinkle orientation was affected in the region within approximately 3 μm (or 20λ) from both edges of the 25 μm line.

In summary, we have demonstrated that polymer nanowrinkles could reach high aspect ratios (>1) and could be oriented by controlling and patterning strain in the skin layer.

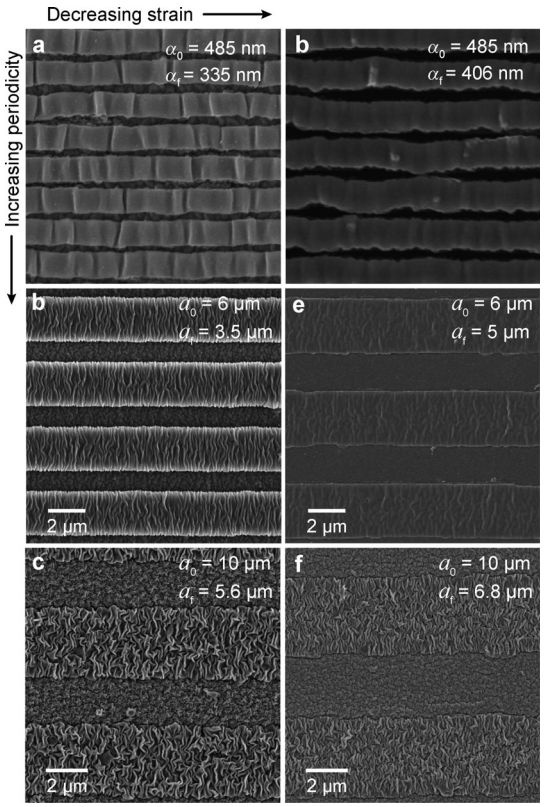

Figure 5. Orientation of wrinkles perpendicular to patterned lines of strain relief over large distances. SEM images of nanowrinkle samples with line arrays of strain-relief features with the periodicities indicated. a) $a_0 = 485$ nm, $a_f = 335$ nm; b) $a_0 = 6$ μm, $a_f = 3.5$ μm; c) $a_0 = 10$ μm, $a_f = 5.6$ μm; d) $a_0 = 485$ nm, $a_f = 406$ nm; e) $a_0 = 6$ μm, $a_f = 5$ μm; f) $a_0 = 10$ μm, $a_f = 6.8$ μm.

We found that adjusting the macroscale strain could produce two types of secondary structures, self-similar wrinkles and nanofolds. By matching the periodicity of strain-relief features with nanowrinkle wavelength, we induced the formation of folds with specific periodicities and orientations. Since nanowrinkles and nanofolds spontaneously form across the entire surface, our study provides a parallel method to create complex ordered and disordered patterns with nanoscale resolution. We anticipate that this investigation will facilitate a physical understanding of the mechanism of the formation of wrinkles and folds and provide a platform for incorporating these nanotextures into new devices.

Experimental Section

Fabrication of 2D nanowrinkles: PS films were treated with a plasma in a RIE system (Samco) for different exposure times (typically 30 s) with the gas CHF_3 at a flow rate of 25 sccm, at a power of 70 W and a pressure of 20 Pa. The chemically treated PS was then heated in a convection oven at 130 °C until the films had shrunk to the desired size. For 2D nanowrinkles, the strain was determined by measuring the area of a box drawn on the substrate before and after shrinking and using the equation $\varepsilon = (A_0 - A_f)/A_0$, in which A_0 is the initial area and A_f is the final area. For 1D samples, the strain was determined from the change in distance between two lines drawn on the sample before and after the final shrinking by using the equation $\varepsilon = (l_0 - l_f)/l_0$, in which l_f is the final length, and l_0 is the initial length. Nanowrinkle surfaces were then coated with a layer of AuPd with a thickness of approximately 8 nm for SEM imaging.

Fabrication of strain-relief patterns: Composite poly(dimethylsiloxane) masks patterned with arrays of recessed posts or lines were prepared for inverse solvent-assisted nanoscale embossing (inSANE).[23] Directed nanowrinkle surfaces on PS films were created by: 1) patterning of the top of the PS films with photoresist in ethanol by inSANE; 2) treatment of the PS films with a plasma in a RIE system (Samco) for different exposure times (typically 30 s) with SF_6 or CHF_3 as the gas at a flow rate of 20 sccm, and at a power of 70 W and a pressure of 20 Pa; 3) deposition of a thin (4 nm) layer of Cr by using an electron beam deposition system and lifting off of the photoresist by the use of isopropanol; 4) treatment of the PS films with a plasma in a RIE system (Samco) for 30 s with the gases Ar (30 sccm) and O_2 (5 sccm) at 70 W and 20 Pa; and 5) removal of Cr with chromium etchant (Transene Company Inc.) and heating of the PS in a convection oven at 130 °C until the films had shrunk to the desired size.

Received: April 19, 2014
Published online: July 1, 2014

Keywords: materials science · nanofolds · nanowrinkles · polymers · reactive ion etching

[1] J. Genzer, J. Groenewold, *Soft Matter* **2006**, *2*, 310.
[2] N. Bowden, S. Brittain, A. G. Evans, J. W. Hutchinson, G. M. Whitesides, *Nature* **1998**, *393*, 146.
[3] B. Li, Y. P. Cao, X. Q. Feng, H. J. Gao, *Soft Matter* **2012**, *8*, 5728.
[4] K. Efimenko, M. Rackaitis, E. Manias, A. Vaziri, L. Mahadevan, J. Genzer, *Nat. Mater.* **2005**, *4*, 293.
[5] P. Kim, M. Abkarian, H. A. Stone, *Nat. Mater.* **2011**, *10*, 952.
[6] C. C. Fu, A. Grimes, M. Long, C. G. L. Ferri, B. D. Rich, S. Ghosh, S. Ghosh, L. P. Lee, A. Gopinathan, M. Khine, *Adv. Mater.* **2009**, *21*, 4472.
[7] L. Pocivavsek, R. Dellsy, A. Kern, S. Johnson, B. Lin, K. Y. Lee, E. Cerda, *Science* **2008**, *320*, 912.
[8] J. Y. Chung, J. P. Youngblood, C. M. Stafford, *Soft Matter* **2007**, *3*, 1163.
[9] M. D. Huntington, C. J. Engel, A. J. Hryn, T. W. Odom, *ACS Appl. Mater. Interfaces* **2013**, *5*, 6438.
[10] J. B. Kim, P. Kim, N. C. Pegard, S. J. Oh, C. R. Kagan, J. W. Fleischer, H. A. Stone, Y.-L. Loo, *Nat. Photonics* **2012**, *6*, 327.
[11] F. Brau, H. Vandeparre, A. Sabbah, C. Poulard, A. Boudaoud, P. Damman, *Nat. Phys.* **2011**, *7*, 56.
[12] N. Bowden, W. T. S. Huck, K. E. Paul, G. M. Whitesides, *Appl. Phys. Lett.* **1999**, *75*, 2557.
[13] Q. H. Wang, Y. J. Yin, H. M. Xie, J. Liu, W. Y. Yang, P. W. Chen, Q. M. Zhang, *Soft Matter* **2011**, *7*, 2888.
[14] P. C. Lin, S. Yang, *Appl. Phys. Lett.* **2007**, *90*, 241903.
[15] M.-W. Moon, S. H. Lee, J.-Y. Sun, K. H. Oh, A. Vaziri, J. W. Hutchinson, *Proc. Natl. Acad. Sci. USA* **2007**, *104*, 1130.
[16] D. B. H. Chua, H. T. Ng, S. F. Y. Li, *Appl. Phys. Lett.* **2000**, *76*, 721.
[17] J.-H. Lee, H. W. Ro, R. Huang, P. Lemaillet, T. A. Germer, C. L. Soles, C. M. Stafford, *Nano Lett.* **2012**, *12*, 5995.
[18] N. Uchida, *Physica D: Nonlinear Phenomena* **2005**, *205*, 267.
[19] Q. Wang, X. Zhao, *J. Appl. Mech.* **2014**, *81*, 051004.
[20] F. A. Bayley, J. L. Liao, P. N. Stavrinou, A. Chiche, J. T. Cabral, *Soft Matter* **2014**, *10*, 1155.
[21] F. Brau, P. Damman, H. Diamant, T. A. Witten, *Soft Matter* **2013**, *9*, 8177.
[22] D. J. Plazek, *J. Phys. Chem.* **1965**, *69*, 3480.
[23] M. H. Lee, M. D. Huntington, W. Zhou, J. C. Yang, T. W. Odom, *Nano Lett.* **2011**, *11*, 311.

